

Optimizing Facies Analysis, Capillary Pressure, and Flow Units Identification of Mishrif Carbonate Reservoir in a Selected Oilfield, Southern Iraq

Mohammed Abdullah Khashman¹, Hamed Shirazi¹, Ahmed N. AL-Dujaili*², Nada M. Sulaiman³

¹ Reservoir Engineering Department/Faculty of Petroleum and Chemical Engineering, Islamic Azad University, Science and Research Branch shohada Hesarak blvd, I.R. Iran

² Amirkabir University of Technology/ Petroleum Engineering Department, Tehran, I.R. Iran

³ Petroleum Engineering Department College of Engineering/ University of Baghdad, Al-Jadriya - Baghdad, Iraq

Received January 31, 2024; Accepted May 12, 2024

Abstract

The Mishrif carbonate reservoir stands out as a crucial hydrocarbon source in the South of Iraq, comprising deposits from the Tertiary and Upper Cretaceous periods. This research delves into the rock characteristics utilizing methods such as flow unit classification (FZI), the Winland approach, and the Stratigraphic Modified Lorenz Plot (SMLP) utilizing core data. Subsequently, it involves capillary pressure (Pc) estimation through laboratory Pc curves and the calibration of different fluid systems for the two wells in the simulator. Findings from this investigation revealed that the Mishrif Formation exhibits four primary facies: predominantly high porosity-permeability facies, followed by medium to high, low to medium, and low porosity-permeability facies, with Megapores and Macropores being dominant rock features. The modified Lorenz plot based on stratigraphy displays 19 distinct flow units. Capillary pressure curves typically fall within 12% to 40% of saturation, representing three reservoir facies: extremely high, high, and medium performing. The majority of hydrocarbons are associated with the MB11 and MB21 units.

Keywords: Mishrif formation; Facies analysis; Rock type; Flow zone indicator; Capillary pressure.

1. Introduction

Petrophysics involves the raw data interpretation from oil and gas reservoirs to define lithology, volume, and other properties [1-2]. These data aid in comprehending the relationships between rock and fluids within the reservoir, leading to a thorough understanding of the reservoir itself. It is instrumental in constructing simulation models for oil and gas reservoirs [3-5]. Utilizing terms like Rock-typing, Flow unit, and electrofacies plays a pivotal role in developing models for interpreting reservoir characteristics. These detailed 3D models incorporate geological traits, petrophysical aspects, and dynamic behavior [6-8]. The economic evaluation of oil reservoirs hinges on critical features such as geological facies, porosity (Φ), permeability (K), water saturation (Sw), and reservoir heterogeneity. Defining and quantifying these parameters is vital for efficient reservoir management and economic viability.

Flow units and rock typing are essential in identifying similar petrophysical zones within heterogeneous reservoirs, contributing to well zonation based on consistent flow patterns [9]. These characteristics represent continuous intervals in the reservoirs, each characterized by distinct flow performance and geological features of rock types. By considering the reservoir's stratigraphic framework, flow units and rock typing aid in a more comprehensive understanding of its flow behavior and facilitate effective reservoir management [10]. Figure 1 outlines the comprehensive process of petrophysical rock typing, starting from core sampling and culminating in flow unit identification. Log profiles like the GR log offer a detailed view of the

well's geological layers. Establishing connections between mineral composition, stratigraphy, seismic data, and other factors is crucial for understanding production mechanisms thoroughly [11]. The characterization process can be divided into various stages, with the Petrophysical Integration Process Model (PIMP) outlining four essential stages within this framework [12]:

- Phase I (Geological assessment): Assess geological characteristics and establish the broad-scale structure and geometry.
- Phase II (Petrophysical assessment): Analyze the rock and fluid systems at a microscopic scale.
- Phase III (Formation analysis): Integrate the insights gathered from Phases One and Two and represent the reservoir using upscaling methods.
- Phase IV (Reservoir or Dynamic modeling): Align the geological and petrophysical models developed in the prior phases and generate both 2D and 3D representations of wellbores and the reservoir.

Integrating geological, petrophysical, and dynamic properties of rocks poses an important challenge in identifying rock types, mainly in complex porosity carbonate reservoir models [13].

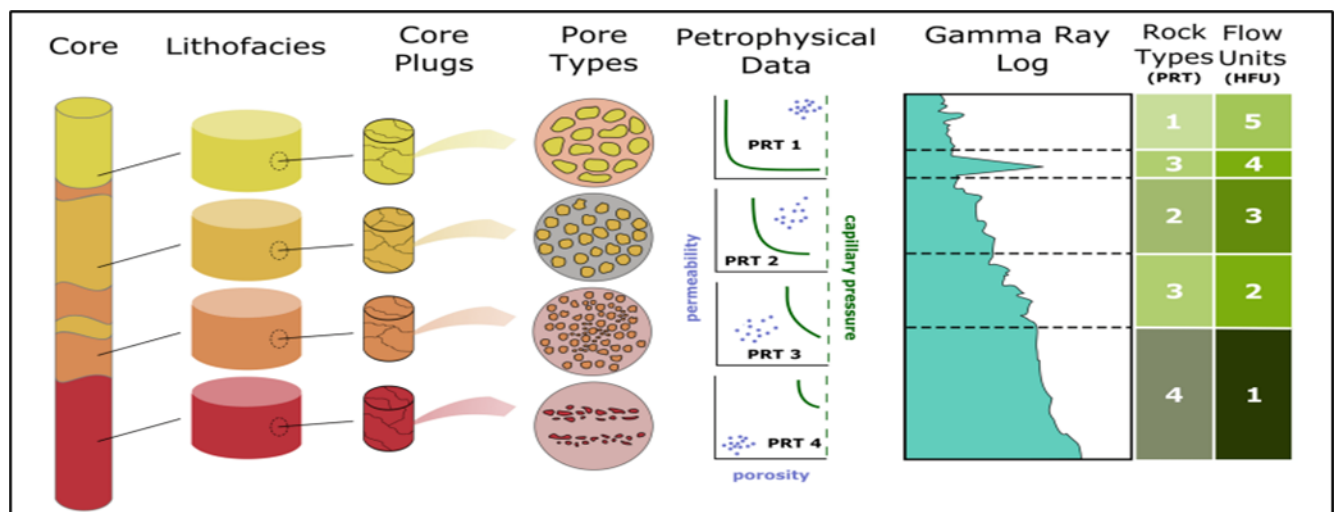


Fig. 1. The condensed procedure for petrophysical rock typing. A link between the flow characteristics and geological attributes by amalgamating core observations with lithofacies, pore classifications, rock-fluid information, well logs, rock categories, and flow unit assessments (modified from [14]).

The study focuses on rock-type classification methods and explores how clustering techniques can enhance rock differentiation [15]. The primary aim is to gather essential insights for developing an optimized reservoir model in challenging reservoir conditions and understanding the behavior of identified rock types when integrating petrophysical and geological attributes. Additionally, the research aims to identify geological factors influencing rock-type formation. Various established methodologies like Winland R35 [16], FZI, [17-18], and SMLP [19], will be employed to achieve these objectives and to determine the most appropriate approach for the specific reservoir under study. Moreover, different clustering approaches, such as the discrete Rock Type (DRT), Probability, and the standard chart, will be applied strategically to define flow unit boundaries within the reservoir.

After this, adjusting capillary pressure (P_c) for each rock type, derived from Flow zone indicators using laboratory P_c curves in simulators, will be necessary due to variations in fluid systems (e.g., air-brine in the lab versus oil-brine in the reservoir). This comprehensive strategy will yield valuable information on reservoir rock characterization, enabling informed decisions for reservoir management and production optimization.

1.1. Rock typing methods

Rock typing methods are techniques used to categorize reservoir rocks based on various petrophysical and geological properties. The purpose of rock typing is to group rocks with

similar characteristics, which can be important in reservoir characterization and management. A method using hydraulic flow units (HFUs) was presented to define rock Facies due to significant permeability variation within well-defined rock types [20].

In this study, HFU identification was accomplished by classifying the reservoir based on its cumulative flowing capacity, employing the SMLP method [19]. Meanwhile, Petrophysical Rock Types (PRT) identification relied on the FZI (Flow Zone Indicator) and Winland R35 methods. Additionally, capillary pressure measurements using mercury injection were applied to characterize each petrophysical rock type based on its capillary pressure behavior. Some common rock typing methods include:

1.2. Hydraulic flow units (HFUs)

Hydraulic flow units (HFUs) are specific zones within a reservoir that significantly impact the flow of fluids and can be interconnected and geographically depicted. These HFUs are intimately associated with flow zone indicators (FZI), which represent unique parameters characterizing each hydraulic flow unit. The connection between reservoir quality indexes (RQI), FZI, and void ratio (ϕ_z , representing the ratio of pore volume to solid volume) is articulated as follows [20]:

$$\text{Log RQI} = \text{Log FZI} + \text{Log } \phi_z \quad (1)$$

$$\phi_z = \left[\frac{\phi_e}{(1 - \phi_e)} \right] \quad (2)$$

Reservoir Quality Index and Flow Zone Indicator can be calculated using the following equations:

$$\text{RQI} = 0.314 * \sqrt{\frac{k}{\phi_e}} \quad (3)$$

$$\text{FZI} = \frac{\text{RQI}}{\phi_z} \quad (4)$$

where: FZI: flow zone indicator; RQI: reservoir quality index; μ_m , ϕ_z : normalized porosity (pore volume to grain volume ratio), fraction; ϕ_e : effective porosity, fraction; k : permeability, md; $\sqrt{\frac{k}{\phi_e}}$ called as hydraulic diameter of the rock.

The relationship between ε and RQI is depicted in a semi-log plot of porosity versus permeability [20], and this plot defines the unique porosity-permeability relationship for each hydraulic unit. By storing cored data in hydraulic units with similar FZI values, permeability variations in a reservoir can be better understood based on [20] studies. Hydraulic flow units (HFUs) are defined by classifying log FZI data using various available approaches. An alternative method of flow unit classification is Discrete Rock Type (DRT), which is defined as follows:

$$\text{DRT} = \text{ROUND}(2 \text{LN}(\text{FZI}) + 10) \quad (5)$$

The determination of the number of rock types or hydraulic flow units within the Mishrif Formation was based on the analysis of core samples obtained from two wells in the selected oilfield. These assessments incorporated the utilization of the Reservoir Quality Index (RQI), Flow Zone Indicator (FZI), and a method known as DRT (which employs core data, specifically porosity and permeability, to differentiate the heterogeneity of reservoir rocks).

1.3. Pore throat radius

Winland's (R35) empirical equation, which is based on hydrocarbon storage and flow capacity [21], is used to identify flow units by defining intervals with similar and predictable flow characteristics. Flow units can be recognized through a series of petrophysical cross plots and by calculating the pore throat radii (R35, pore size) at 35% pore volume using Equation 6:

$$\text{Log}(R35) = 0.732 + 0.588 \text{log}(K) - 0.864 \text{log}(\phi) \quad (6)$$

where (R35) is the calculated pore throat radius at 35% mercury saturation from a mercury injection capillary pressure test; K is the permeability (md); and ϕ is porosity (%).

The knowledge of Winland (R35) was to categorize a reservoir into different rock types thus a single rock class with the same R35 will fall on an iso-pore throat curve [22].

1.4. Capillary pressure analysis

Capillary pressure, denoted as p_c , is characterized as the pressure difference between the non-wetting phase and the wetting phase, relative to the wetting-phase saturation [23]. In reservoir engineering, capillary pressure holds significant importance as it is a vital parameter for studying the vertical distribution of saturation within the reservoir. It helps in understanding how fluids are distributed and how they move within the porous rock formations, impacting various aspects of reservoir behavior and production dynamics [24]. Mean parameters exhibit distinctive characteristics in the realm of reservoir analysis. These parameters encompass the connate water saturation transition zone, essential for appraising rock quality, and the pivotal transition zone that governs rock permeability alongside grain assortment. Initially, petroleum reservoirs host water as the primary saturation. Upon oil infiltration, a displacement occurs, replacing the water (wetting phase) with oil (non-wetting phase). Displacement evaluation can be achieved via experimental measurement of the drainage capillary pressure curve in the laboratory tests. When studying reservoirs, modeling water inflow has a crucial significance, making the imbibition capillary pressure a focal point. The imbibition capillary pressure pertains to the process of fluid uptake by the reservoir rock. It provides valuable information on the interactions between the wetting and non-wetting phases during the reservoir's water influx [25].

Several papers have discussed various issues related to the Buzurgan oil field, including facies analysis, capillary pressure, and flow unit classification [26]. In 2022, Al-Husseini and Hamd-Allah explained that understanding the distribution of capillary pressure during drainage processes is essential for determining initial fluid contacts and transition zones in the Mishrif formation of the Buzurgan oil field. [27]. Another by AlHusseini and Hamd-Allah in 2023 revealed that Rock Facies type-3 and 4 had the best petrophysical properties in the high porosity range (14.5% to 18.8%) and low to moderate water saturation range (0.27 to 0.45) [28]. Abdulkareem *et al.* conducted a reservoir simulation for this field and identified the MB21 as the main productive unit in Mishrif Reservoir [29]. Furthermore, the results of Al-Baldawi in 2023 indicated that the Mishrif Formation has four distinct rock types with varying reservoir qualities [30]. In the Halfaya oil field, which is near the Buzurgan, an integrated analysis of well-loggings and 3D seismic records of the Mishrif Formation revealed the presence of five lithofacies associations [31]:

1. Subtidal mudstone to wackestone (LF-1).
2. Back-margin massive wackestone to packstone (LF-2).
3. High-energy bioclastic grainstone (LF-3).
4. Swamp carbonaceous mudstone interbedded with bioclastic wackestone (LF-4).
5. Incision brown mudstone to wackestone with chert nodular (LF-5).

The result of Liu *et al.*, for petrophysical static rock typing for carbonate reservoirs based on mercury injection capillary pressure curves using principal component analysis showed that the MICP curve evaluation is irrelevant to the number of characteristic parameters but closely related to the characteristic parameters [32].

This study aims to develop a better understanding of Facies, Capillary Pressure, and Flow Units Identification of the Mishrif formation in southeastern Iraq, particularly in the Buzurgan oil field.

1.5. Geological setting

Carbonate sequences are a globally significant hydrocarbon resource. In the lower Cretaceous, the Mishrif Formation is positioned between the Khasib Formation above and the Rumaila Formation below [33]. At this particular oilfield, the lithology of the Mishrif Formation primarily consists of limestone and dolomite, interspersed with layers of shale. Furthermore, the Mishrif Formation is subdivided into three units denoted as MA, MB, and MC. Figure 2 provides a stratigraphic column of Iraq, detailing age and lithology descriptions. The Mishrif Formation exhibits notable variations in lithology, porosity, and permeability, contributing to reservoir heterogeneity and influencing the flow of oil and gas in the field [34]. In the Amara,

Halfaiya, Majnoon, and Buzurgan areas, the Mishrif Formation measures approximately 350 to 400 meters in thickness but thins to the southwest. It is most prominently developed as substantial rudist buildups atop structural highs in Southern Iraq, particularly within the eastern Mesopotamian Zone [35].

	Age	Formation	Lithology	Note	
Tertiary	Pliocene	Bakhtiary	Marly clay + Gypsum + Sandy clay		
	Upper Miocene	Upper Fars	Gravel Sand + Siltstone + Anhydrite + Shale		
	Middle Miocene	Lower Fars – MB5		Shale + Anhydrite + Limestone + Dolomite	
		Lower Fars – MB4		Shale + Anhydrite + Salt + Limestone	
		Lower Fars – MB3		Anhydrite + Salt + Shale	
		Lower Fars – MB2		Salt	
		Lower Fars – MB1		Anhydrite + Shale + Dolomite	
	Burdigalian	Jeribe/Euphrates	Limestone + Dolomite		
	Aquitanian to Oligocene	Upper Kirkuk		Sand + Siltstone + Shale + Dolomite	Asmari Formation
		M-L Kirkuk		Sand + Siltstone + Shale	
Eocene to Paleocene	Jaddala		Limestone + Marl + Chert + Shale		
	Aaliji		Marl + Limestone		
Cretaceous	Lower Maastrichtian	Shiranish	Chalky Limestone		
		Hartha	Chalky Limestone		
	Campanian to Santonian	Sadi	Limestone + Marl		
	Coniacian to Turonian	Tanuma	Shale + Marl + Limestone		
		Khasib	Limestone + Shale	Unconformity	
	Lower Turonian to Upper Cenomanian	Mishrif	Limestone		
		Rumaila	Limestone		
	Lower Cenomanian	Ahmedi	Marl + Limestone		
		Mauddud			
	Nahr Umr				

Fig. 2. The stratigraphic column of the Buzurgan oil field, (modified from [46]).

Oil accumulations within the Mishrif Formation reservoir have been located in 32 distinct structures distributed across northern, central, and southern regions of Iraq [36]. The most significant net reservoir thickness is primarily evident within the rudist banks of East Mesopotamia. Porosity levels within this reservoir range from 15% on average, with values reaching as high as 22%. The permeability exhibits a notable degree of variation, with values spanning from 23 to 775 millidarcies (md). The API gravity of the oil extracted from the Mishrif Formation generally falls within a variety ranging from 23 to 36.6 degrees, with an average API gravity of approximately 25 degrees, [37]. The Mishrif Formation is equivalent to several formations in various regions. It corresponds to the upper part of the Massad Formation in the Rutba area [38], additionally, it is comparable to the Jerebi and Merka formations in western Iraq, [39]. This formation also aligns with different geological units in neighbouring countries, such as the Maqwa Formation in Kuwait [40], the Natih Formation member in Oman [41], and the Al-Khatea and Rumaila Formations in the northern UAE, as well as the Salabikh Formation member Schiliaf in Abu Dhabi [42]. In Saudi Arabia, it is situated within the Wasia group [43], and in Iran, it is the stratigraphic equivalent to the upper section of the Sarvak Formation [44]. The Mishrif Formation maintains the same nomenclature in both Qatar and Bahrain [45].

2. Experimental

Rock typing involves classifying reservoir rocks into distinct units that were formed under comparable conditions and underwent similar diagenetic processes. Consequently, each rock type exhibits a consistent porosity-permeability relationship, a uniform capillary pressure profile, and identical water saturation at a specific height above the free water level, as originally outlined [47]. 323 core samples extracted from the Mishrif Formation in the Buzurgan oil field were utilized in this study. These cores cover the whole field parts to make the results more accurate.

Multiple quantitative techniques are available to delineate rock typing and its associated petrophysical characteristics. In this study, various methods were utilized according to the method limitations. These methods were experienced in previous studies for the Mishrif Formation in this area and the Mesopotamia basin and approved that they will be good to analyze (Figure 3). Analyzing facies delves into a comprehensive scrutiny of diverse rock compositions and their unique attributes present in the reservoir. This method involves pinpointing and classifying these facies through cluster analysis aided by IP software. It aims to enhance the spatial mapping of rock properties within the Mishrif Formation in a specified oilfield in Southern Iraq. Such comprehension plays a pivotal role in predicting fluid dynamics within the reservoir and enhancing the efficacy of production tactics.

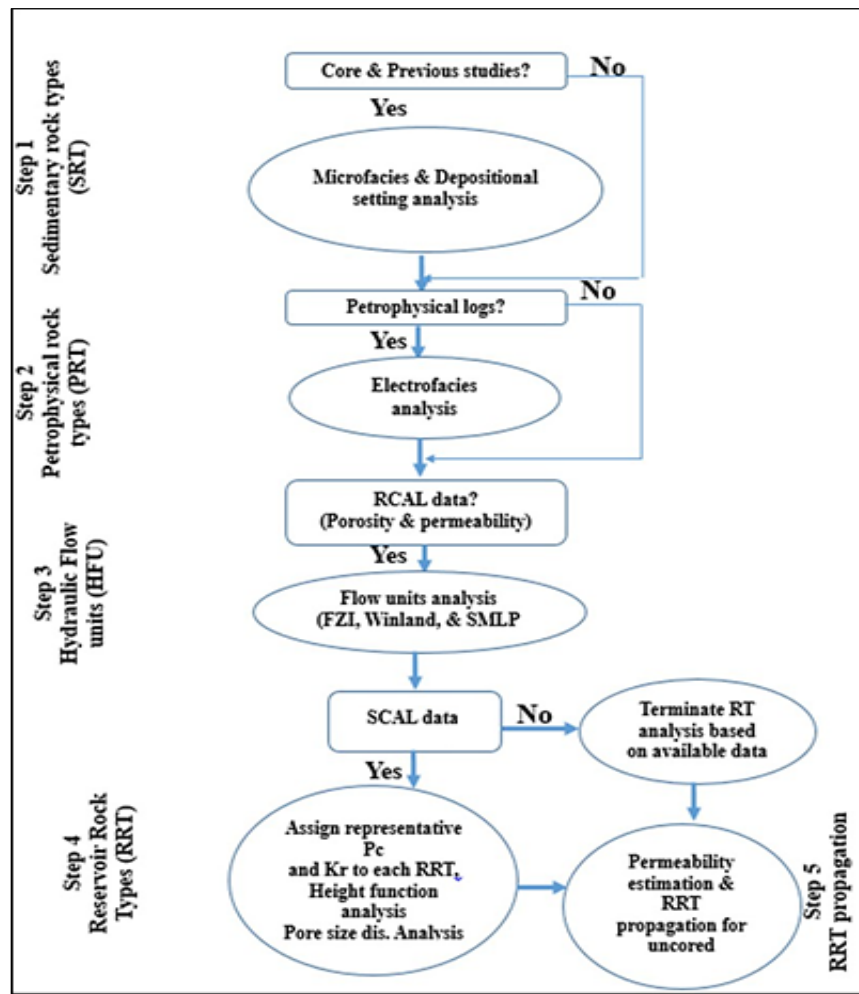


Fig. 3. The workflow for rock typing and the identification of flow units.

Cluster analysis processes are used to identify groups of similar data points in a multi-dimensional log space called electrofacies. These electrofacies can then be used to characterize the physical and fluid properties of rocks in a reservoir. Cluster analysis was utilized to identify unique collections of electrofacies on the response logs of a reservoir. This allowed them to better understand the reservoir's heterogeneity and to develop more effective production strategies. Cluster analysis is a powerful tool for petroleum engineers, as it can help them to better understand the complex geology and Petrophysics of reservoirs [48].

Both raw and interpreted log data, encompassing Gamma Ray (GR), Sonic (DT), Uninvaded Zone (Rt), Invaded Zone (Rxo), Effective Porosity (Φ_e), and Water Saturation (Sw) from fourteen wells, were utilized for cluster analysis. In this research, the data was meticulously input into the Interactive Petrophysics (IP) software. Arranging the datasets involved capturing the logarithmic values, utilizing the K-means statistical technique. This method reduces deviations' sum of squares at individual points. The first phase includes evaluating randomness by determining the mean depth levels per cluster, known as the average cluster thickness, utilizing the initial log information. The theoretical average thickness is calculated to validate if the clusters are uniformly spread across each depth level, as detailed in the specified equations.

$$\text{Avg. thickness} = \frac{\text{Number of depth levels}}{\text{Number of cluster layers}} \quad (7)$$

$$\text{Random thickness} = \sum \frac{P_i}{(1 - P_i)} \quad (8)$$

where p_i is the proportion of the depth of the cluster allocated.

$$\text{Randomness index} = \frac{\text{Avg. Thickness}}{\text{Random Thickness}} \quad (9)$$

The rock types were classified based on their pore radius (R35) values, following the criteria [49]:

- Megapores: When R35 exceeds 10 μm , the rock is categorized as a "Megapores" and can yield production rates in the range of tens of thousands of barrels per day.
- Macropores: A rock is designated as "Macropores" when R35 falls within the range of 2 to 10 μm , with the potential to yield several hundred barrels per day.
- Mesopores: A rock is characterized as "Mesopores" when R35 falls in the range of 0.5 to 2 μm and can support production levels in the hundreds of barrels per day.
- Micropores: Rock types with pore radius (R35) values within the range of 0.1 to 0.5 μm .
- Nanopores: Rock types with pore radius (R35) values less than 0.1 μm .

The Stratigraphic Modified Lorenz Plot (SMLP) method is a proper technique for determining flow attributes within porous media. SMLP illustrates the relationship between cumulative flow capacity (cumulative %Kh) and cumulative storage capacity (cumulative %K Φ) in the reservoir's stratigraphic sequence to define petrophysical flow units within wells. By plotting cumulative storage and flow capacity on a Lorenz diagram in stratigraphic order, changes in slope can indicate variations in flow behavior. Steep segments of the plot suggest high reservoir flow capacity relative to storage capacity, potentially indicating efficient flow conduits or faster reservoir processes.

Alternatively, barriers or seals within the porous medium can appear as segments devoid of storage and flow capacity. Meanwhile, baffles represent regions with limited flow capacity relative to storage capacity. The SMLP method could be valuable for identifying rock types based on their flow behavior [50]. The construction of the SMLP and MLP (Modified Lorenz Plot) entails five distinct steps.

- 1) Organizing the data by depth.
- 2) Calculating the proportions of storage and flow capacity for each data point in Routine core analysis (RCA) through the "Phi depth" and "Permeability depth" variables.
- 3) Generating the Stratigraphy-based Modified Lorenz Plot (SMLP) by plotting the percentages of storage capacity against flow capacity. Each inflection point serves to identify initial flow units.
- 4) Confirming and finalizing each initial flow unit by cross-validating it with various other methodologies such as SFP (Stratigraphic Flow Path), Winland, RQI/FZI (Reservoir Quality

Index/Flow Zone Indicator), and BVW (Bulk Volume Water) across the entire wellbore within the reservoir column.

5) Constructing the Modified Lorenz Plot (MLP) to represent the final flow units, organized by their decreasing flow speed.

Air-brine capillary pressure data for Mishrif Formation was available from plugs using the Porous Plate method/ spontaneous imbibition for (Well-1 & Well-2). The plugs had permeabilities in the range <10 mD to 102 mD, and porosities 12 % to 25%. This adequately covered the observed range in the data. All necessary corrections were achieved including Stress, clay-bound water, and fluid correction to adjust the results from the laboratory to reservoir conditions.

The laboratory Pc curves were utilized in the simulator adjustment to be made for the different fluid systems, i.e. air-brine in the laboratory Vs oil-brine in the reservoir, this is normally handled through the Leverett J-function, defined as given in Equation [51]:

$$J(S_w) = \frac{P_c}{(\sigma \cdot \cos \theta) * \sqrt{\frac{K}{\phi}}} \quad (10)$$

All capillary pressure data falling within the water saturation classes was plotted out on a normalized saturation scale, given by following Equation:

$$S_{wn} = \frac{(S_w - S_{wc})}{(1 - S_{wc})} \quad (11)$$

De-normalized water saturation can be found from this equation:

$$S_w = S_{wn} * (1 - S_{wc}) + S_{wc} \quad (12)$$

3. Results and discussion

3.1 Cluster analysis

The plot is constructed by selecting the clusters with the least randomness, typically denoted by the highest points. This is done after introducing some noise, aiming to replace a high level of randomness with an average level. The degree of randomness is quantified using values, with greater values [52]. The randomness plot specific to the Mishrif Formation is visually depicted in Figure 4.

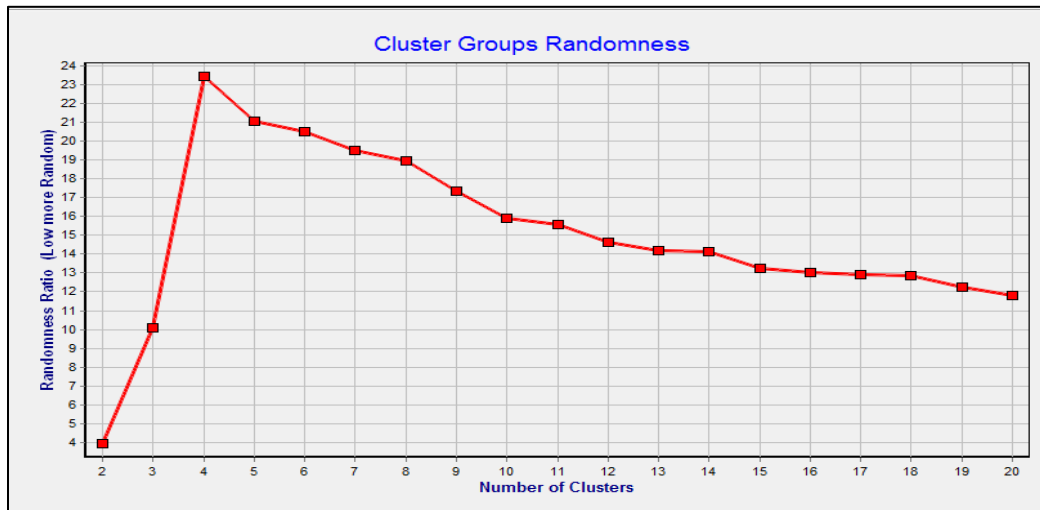


Fig. 4. Randomness Assessment of Cluster Group Types within the Mishrif Formation.

To classify a new data point (rock facies attribute vector) is presented by SOM. Self-Organizing Maps (SOMs) offer an effective way to classify rock facies based on their attributes and capture the spatial relationships and patterns in geological formations. They provide a graphical representation of the data distribution, aiding geoscientists in understanding and interpreting complex geological structures. Additionally, SOMs can be valuable for exploring data and identifying potential new facies or stratigraphic features that may not have been apparent

through traditional methods. Figure 5 depicts the ultimate graphical representation of the cluster analysis conducted on fourteen wells within the Mishrif Formation.

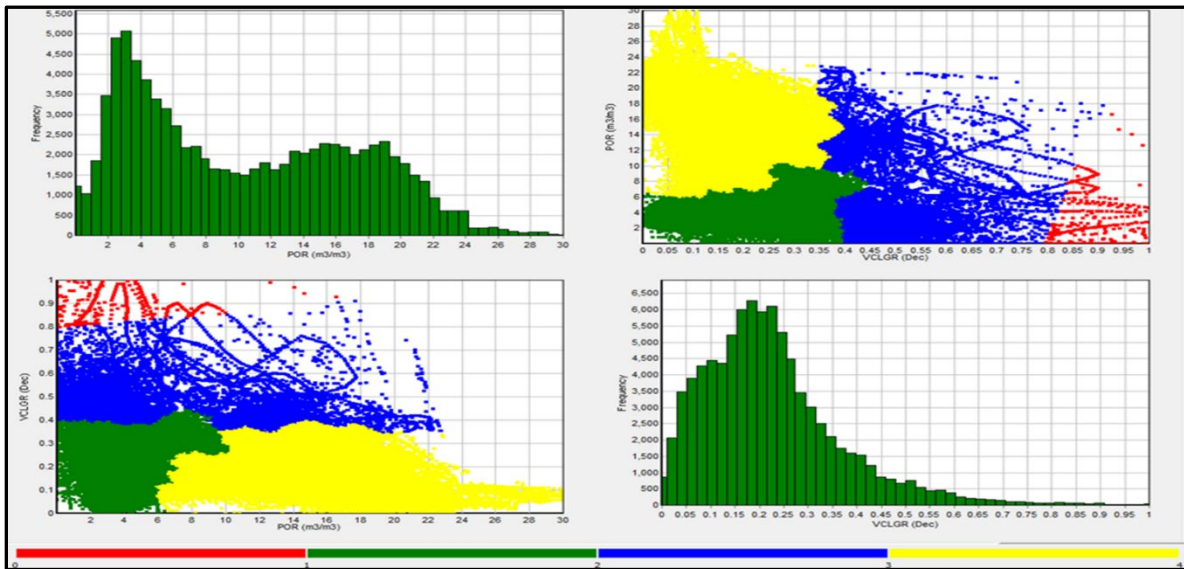


Fig. 5. Plot of cluster editing result.

The cluster analysis technique identified four distinct rock types, which are further described below and visualized in Figure 6:

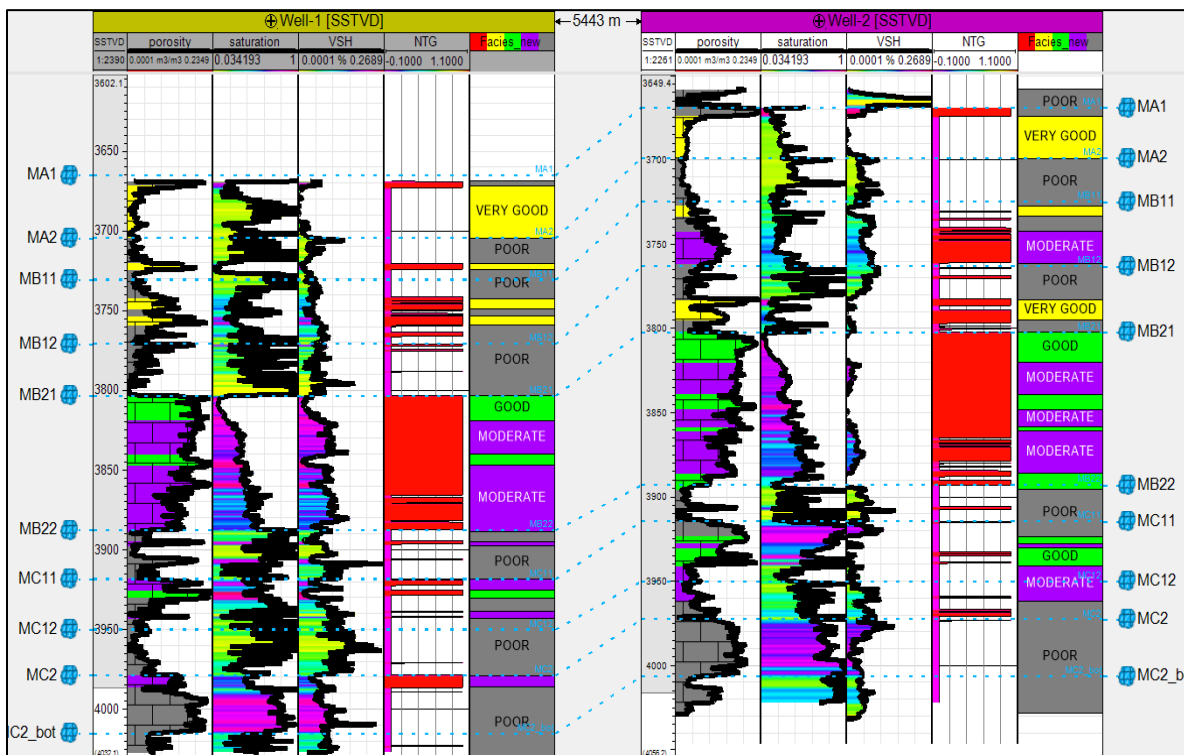


Fig. 6. A cross-sectional representation of rock types within the Mishrif Formation for wells 1 and 2 using Cluster Analysis.

- 1) Rock Type-I: This category represents the highest quality type (displayed by the yellow), and it is categorized by the low GR and water saturation values, and values of the neutron, sonic, and R_t were notably greater than R_{xo} , which lead to high porosity values.

- 2) Rock Type-II: This type is considered a good quality (displayed in blue). It exhibits low GR and modest water saturation values and medium to-great values of neutron, sonic, and Rt, which are higher than Rxo. Porosity values in this category are medium to high.
- 3) Rock Type-III: Occupying the intermediate classification (displayed in green). This type is characterized by moderate GR and water saturation values and intermediate for neutron, sonic, and Rt, which exceed Rxo, and the porosity values in this category are low to medium, signifying mid-range characteristics.
- 4) Rock Type-IV: Represents the least favorable rock type (marked in red). It features high GR and water saturation values and low for neutron, sonic, and Rt, slightly less than Rxo. The porosity in this category isn't exceptionally low.

According to Net-to-gross (NTG) calculations, hydrocarbons lie in the MB11 and MB21 units mainly (Figure 6).

3.2. Flow units

This method identified unique FZI ranges for various rock types within the Mishrif Formation, which leads to their classification into four distinct categories, as shown in Figures 7 and 8. The quality of different rock types was evaluated based on DRT criteria outlined in Table 1. A power model was employed to graphically represent the relationship between permeability and porosity for each rock type, displaying strong correlation coefficients across the board. As a result, accurate estimations of permeability based on the porosity values specific to each rock type are attainable.

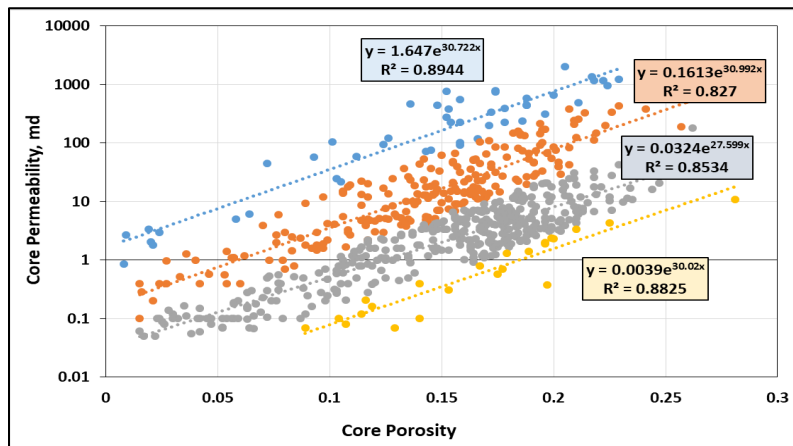


Fig. 7. Core Porosity Vs. Core Permeability for Mishrif Formation.

Table 1. Rock types and corresponding DRT and FZI.

Rock Code	Rock type	DRT-range	FZI-range
1	Rock Type-I	13- 16	3.881-11.6744
2	Rock Type-II	11 -13	1.461-2.898
3	Rock Type-III	9 -11	0.4183-1.66
4	Rock Type-IV	7- 9	0.1562-0.4752

Through core analysis, the permeability values varied across the range from 0.05 md to 1367 md, with an average value of 46.078 md. The permeability estimation is based on the porosity-permeability relationship specific to each rock type. Four rock types were delineated using the DRT criterion, as visually demonstrated in Figures 9 and 10. These equations serve as a valuable resource for estimating permeability within the geological model, with each rock type's unique permeability equation detailed in Table 2.

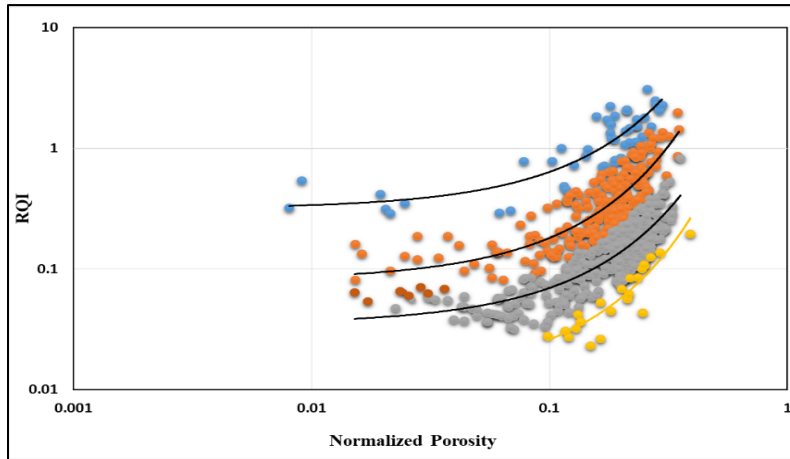


Fig. 8. Relationship between rock quality index (RQI) versus normalized porosity (PHIZ).

Table 2. Rock classification and correlations within the Mishrif Formation.

Rock Code	Rock type	Correlations	Correlation coefficient R ²
1	Rock Type-I	$K=1.647 * e^{(30.722 * \phi)}$	0.8944
2	Rock Type-II	$K=0.1613 * e^{(30.992 * \phi)}$	0.827
3	Rock Type-III	$K=0.0324 * e^{(27.599 * \phi)}$	0.8534
4	Rock Type-IV	$K=0.0039 * e^{(30.02 * \phi)}$	0.8825

The outcomes of this approach reveal that the Mishrif Formation can be categorized into four distinct hydraulic flow units (HFUs). Each HFU exhibits consistent FZI ranges and signifies a unique rock type characterized by varying porosity and permeability attributes. These HFU groupings are as follows:

- HFU-I: This group reflects a very good porosity-permeability trend and represents the reservoir rock with best quality in the Mishrif Formation.
- HFU-II: This group reflects a good porosity-permeability trend and represents good reservoir rock quality.
- HFU-III: This group reflects a moderate porosity-permeability trend and represents the intermediate reservoir rock quality.
- HFU-IV: this group reflects a low porosity-permeability trend and represents bad reservoir rock quality.

The correlation recognized by Winland was applied to identify different types of rock or HFU in the Mishrif Formation based on the permeability and porosity values. The pore radius (R35) or pore type using the available core data of Well-1 and Well-2 was identified, where four pore size groups or HFUs have been recognized in Fig.9 and described as follows:

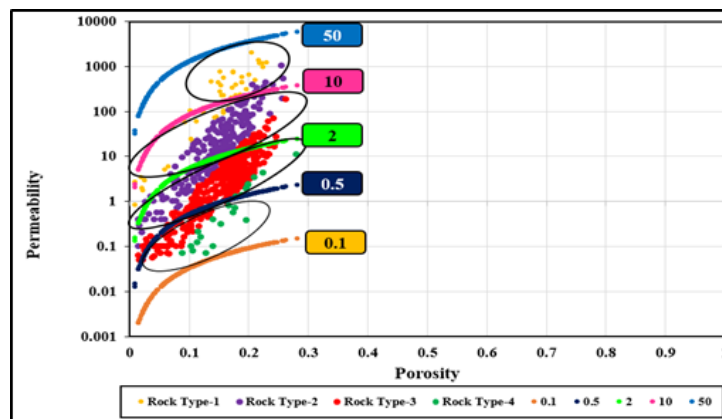


Fig. 9. Relationship between core porosity and core permeability of (R35 Method).

3.3. Rock type

Utilizing the available core analysis data, which includes porosity and permeability, we have identified different pore types and their respective pore radius (R35). Four distinct groups of pore sizes have been distinguished, as illustrated in Figure 9.

- Megapores Type: This signifies a high-quality reservoir rock type, corresponding to the first group of the Flow Zone Indicator (HFU-I).
- Macropores Type: Represents a good reservoir rock quality, aligning with the second group of the Flow Zone Indicator (HFU-II).
- Mesopores Type: Indicates an intermediate reservoir rock quality, corresponding with the third group of the Flow Zone Indicator (HFU-III).
- Micropores Type: Denotes lower reservoir quality and corresponds with the fourth group of the Flow Zone Indicator (HFU-IV).

3.4. Stratigraphic modified Lorenz plot (SMLP) method

The implementation of these steps enables the recognition and thorough characterization of flow patterns within the reservoir. Figures 10, 11, and 12 offer visual depictions of the Stratigraphy-based Modified Lorenz Plot (SMLP) and the Modified Lorenz Plot (MLP) for two wells. Inflection points show the flow changes or storage capacity, which help to evaluate reservoir flow. Steeper slopes indicate faster flow rates, while horizontal trends indicate little to no flow. The consistent 45° trend of the storage capacity line suggests that storage capacity is evenly distributed throughout the reservoir. When the two lines overlap or closely follow each other, all pores contribute equally to flow; this trend could result from inter-crystalline or inter-particle porosity. As the lines separate, different pores contribute more to flow than moldic or vuggy porosity would indicate. Examination of the inflection points within the SMLP curves has resulted in the identification of a total of 19 distinct flow units.

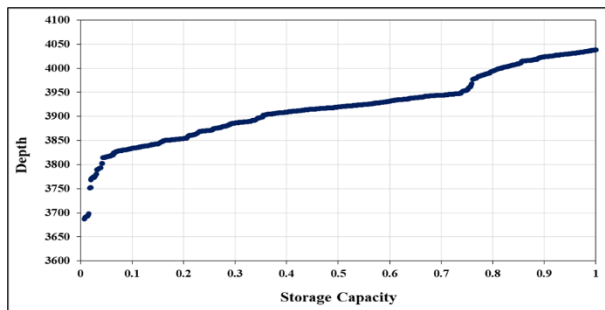


Fig. 10. Relationship of storage capacity with depth.

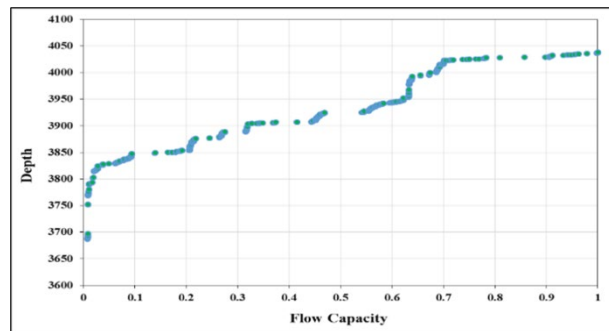


Fig. 11. Relationship of flow capacity with depth.

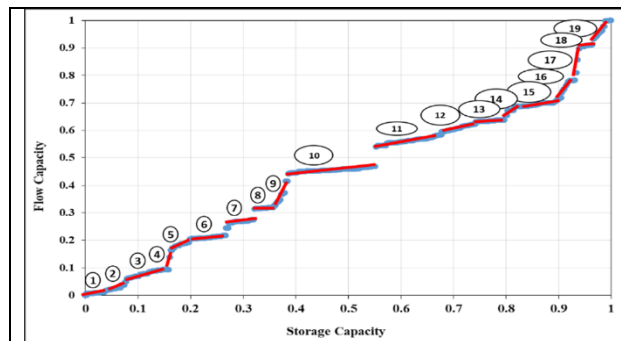


Fig. 12. Relationship of storage capacity with flow capacity.

The Flow Capacity (permeability multiplied by thickness) is plotted against the Storage Capacity (porosity multiplied by thickness). The Stratigraphic Modified Lorenz Plot (SMLP) is a graphical tool employed to discern distinct flow standards within a reservoir concerning storage and flow capacities. It proves particularly valuable in determining the minimum number of hydraulic flow standards.

The creation of the SMLP, as depicted in Figure 12, involves the utilization of core data measurements to calculate storage capacity (as illustrated in Figure 10) and flow capacity (as shown in Figure 11) within the stratigraphic framework, including the cumulative percentage of sample interval points by depth.

The resulting plot shows different hydraulic flow standards, marked by inflection points along the curve.

For example, in Figure 12, the data reveals the presence of 19 distinct hydraulic flow standards. The steeper the slope of a line segment (e.g., segments 4, 9, and 17 in Figure 12), the greater the flow capacity of the corresponding depth segment, while a flatter line segment (e.g., segments 6, 8, 10, and 18 in Figure 12) indicates poorer flow capacity in the respective

3.5. Air-brine capillary pressure

A plot of the laboratory data (Figure 13), which the curves have been color-coded according to the Water saturation class detailed below in Table (3).

Table 3. Water saturation classes.

Group	Water saturation range
1	$S_w < 20$
2	$20 \leq S_w < 30$
3	$30 \leq S_w < 50$
4	$S_w > 50$

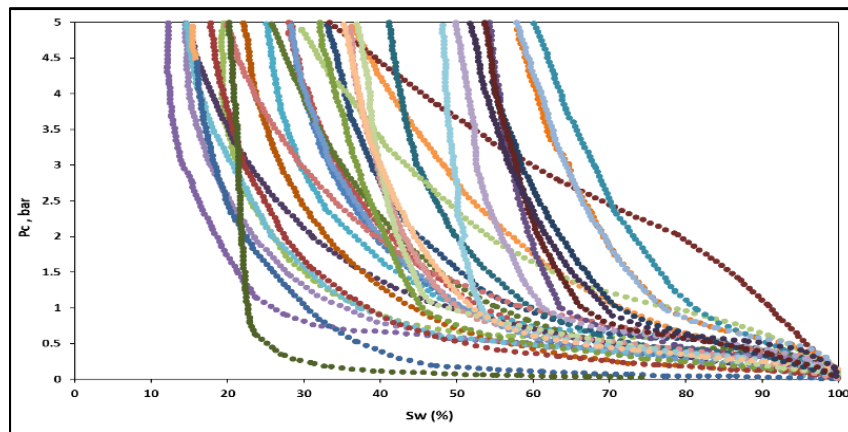


Fig. 13. Capillary Pressure of all samples of Mishrif Formation.

3.6. Capillary pressure procedure

The differing curves attempted to reflect a slight difference in shape to the saturation profile observed through the transition zone. The final curves entered into the simulator require the J-function to be entered. So that the simulator can back calculate a capillary pressure curve for each grid cell (Figure 14).

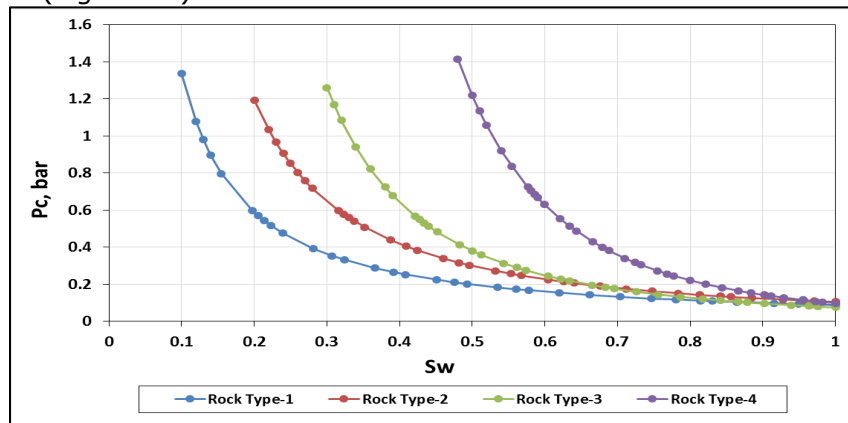


Fig. 14. Capillary pressure of each rock type.

3.7. Discussion

The MA HFLs are characterized by low porosity / high permeability / high resistivity. They are generally observed around faults where diagenesis and/or fracturing enhance their flow properties. Because of its high permeability, the impact on water breakthrough and the significant under-sampling of these facies in the core, further data acquisition is required (core, FMI, dipole sonic) to describe the flow properties of these facies better. These rocks in MA are distinguished by their capability to yield free oil, featuring a high oil column, a water saturation range of less than 20%, coarse porosity, substantial porous throat dimensions, and elevated oil saturation.

The mB1 does not represent a significant reservoir of porous rocks with a high porosity. An amount of oil in good reservoir quality rocks or rocks with tight platform facies existed. Relatively to the Microporous rocks with a high porosity elsewhere in the Mishrif that provide an attractive development opportunity, the poorer reservoir quality in mB1 represents a much poorer development opportunity. These facies of MB1 are marked by the extraction of free oil, a high oil column but porous system featuring moderately sorting a water saturation range ($20 \leq S_w < 30$), and possessing coarse porosity with medium-sized porous throats.

The upper MB2 shows better facies reservoir characterizations with high porosity and low water saturation values than the lower. These facies are identified by their high displacement pressure, and a notable water saturation range ($S_w > 50$), indicative of free water production and a low sorting degree. Facies of the upper MB2 are distinguished by their moderate reservoir quality index, a water saturation range ($30 \leq S_w < 50$), and fine grain size, medium sorting levels, and reduced displacement pressure. Reservoir facies with poor performance can be identified in the lower MB2 and MC. That is according to high saturation values.

Forecasting the performance of rock and reservoir characteristics under varied hydrocarbon recovery scenarios, such as high flow or thief units, and localized barriers or baffles, enables reservoir engineers to identify the safest, most economical, efficient, and most effective development plan for the Mishrif reservoir and will help prioritize efforts and focus on the MB2 and MA units.

Most of the studies that were carried out on the Mishrif Formation, whether in the Buzurgan oil field or the Mesopotamia basin, agreed that this Formation consists of four rock types. This study identified 19 hydraulic flow units for the Mishrif Formation by SMLP and four by RQI methods depending on new data from the cored wells. Al-Jinaay and Jaber [23] could recognize just ten units by the SMLP method and Al-Baldawi four units by the RQI method [27]. The capillary pressure curve in this study showed identical curves more than a study by Liu *et al.*, 2019 [29] and Falah and Alattabi, [24]. That is might due to using the Porous Plate method, which is more accurate than MICP.

According to Air-brine capillary pressure, the most capillary pressure curves lie in the saturation zone between 12 to 40%. That reflects a good reservoir characterization.

4. Conclusions

Reservoir characterization is the crucial initial step in any field development or enhanced oil recovery project. This study aims to offer a comprehensive reservoir description to reduce risks associated with enhanced oil recovery and secondary recovery endeavors. Various methods for characterizing reservoirs and analyzing reservoir rock types and flow units were studied, especially for heterogeneous reservoirs. The cluster analysis of the selected Field reveals that the Mishrif Formation comprises four facies, predominantly high porosity-permeability, followed by medium to high, low to medium, and low porosity-permeability facies. Megapores and Macropores are the prevailing pore throat radii within the Mishrif Formation. Analysis of Stratigraphy-based Modified Lorenz Plot curves has unveiled 19 distinct flow units marked by inflection points. Capillary pressure curves based on Air-brine saturation range between 12% and 40%, highlighting three reservoir facies (Very good, relatively good, and medium performance). The highest reserve of hydrocarbons is in the MB11 and MB21 units.

Mathematical symbols

K	Permeability
P_c	Capillary Pressure
R_{35}	Pore throat radius at 35% mercury saturation
S_w	water saturation
ϕ	porosity
ϕ_e	Effective Porosity

Acronyms and abbreviations

<i>DRT</i>	<i>Distribution of Relaxation Times</i>
<i>DT</i>	<i>Sonic log</i>
<i>FZI</i>	<i>Flow Zone Indicator</i>
<i>GR</i>	<i>Gamma Ray</i>
<i>HFU</i>	<i>High Flow Unit</i>
<i>IP</i>	<i>Interactive Petrophysics</i>
<i>MA</i>	<i>Upper Mishrif</i>
<i>MB1</i>	<i>Lower Mishrif part 1</i>
<i>MB2</i>	<i>Lower Mishrif part 2</i>
<i>MC</i>	<i>Rumaila Formation at base Mishrif.</i>
<i>md</i>	<i>milli-Darcy</i>
<i>MICP</i>	<i>Mercury Injection Capillary Pressure</i>
<i>MLP</i>	<i>Modified Lorenz Plot</i>
<i>PRT</i>	<i>Petrophysical Rock Types</i>
<i>RCA</i>	<i>Routine Core Analysis</i>
<i>RQI</i>	<i>Reservoir Quality Indexes</i>
<i>Rt</i>	<i>Resistivity of uninvaded Zone</i>
<i>Rxo</i>	<i>Resistivity of invaded Zone</i>
<i>SMLP</i>	<i>Stratigraphic Modified Lorenz Plot</i>

Acknowledgement

The authors would like to thank the Islamic Azad University, Science and Research Branch of Petroleum and Chemical Engineering. Also, we appreciate anyone who helped us to make this paper, the executive editor for this journal.

Conflict of interest. There are no conflicts to declare.

References

- [1] Makarian E, Elyasi A, Moghadam RH, Khoramian R, Namazifard P. Rock physics-based analysis to discriminate lithology and pore fluid saturation of carbonate reservoirs: a case study. *Acta Geophysica*, 2023; 71(5): 2163-80. <https://doi.org/10.1007/s11600-023-01029-0>
- [2] Jamali MA, Bissenbay A, Nuraje N. Thermodynamic Modeling and Process Simulation of Kumkol Crude Oil Refining. *Eurasian Chemico-Technological Journal*, 2023; 25(3): 183-92. <https://doi.org/10.18321/ectj1521>
- [3] Gong J, Kang Q, Wu H, Li X, Shi B, Song S. Application and prospects of multi-phase pipeline simulation technology in empowering the intelligent oil and gas fields. *Journal of Pipeline Science and Engineering*, 2023; 3(3): 100127. <https://doi.org/10.1016/j.jpse.2023.100127>
- [4] Tileuberdi, Nurbol, Ahmed N. AL-Dujaili, Moldir Mashrapova, Kuanysh Togizov, Miras Sanatbekov, and Auyelkhan Yergali. "Optimizing oil recovery by low-pressure nitrogen injection: an experiment case study. *ES Materials & Manufacturing*, 2024; 25: 1189. <http://dx.doi.org/10.30919/esmm1189>
- [5] Karimov, D, & Toktarbay Z. Enhanced Oil Recovery: Techniques, Strategies, and Advances. *ES Materials & Manufacturing*, 2023; 23(2): 1005. <http://dx.doi.org/10.30919/esmm1005>
- [6] Lucia FJ. Rock-fabric/petrophysical classification of carbonate pore space for reservoir characterization. *AAPG bulletin*, 1995; 79(9): 1275-1300. <https://doi.org/10.1306/7834D4A4-1721-11D7-8645000102C1865D>
- [7] Al-Dujaili AN. Reservoir and rock characterization for Mishrif Formation/Zubair Field (Rafdiya and Safwan Domes) by nuclear magnetic resonance and cores analysis. *Iraqi Journal of Chemical and Petroleum Engineering*. 2024; 25(3):1-4. <https://doi.org/10.31699/IJCPE.2024.3.1>

- [8] Al-Dujaili AN, Shabani M, AL-Jawad MS. Characterization of flow units, rock and pore types for Mishrif Reservoir in West Qurna oilfield, Southern Iraq by using lithofacies data. *Journal of Petroleum Exploration and Production Technology*, 2021; 11: 4005-18. <https://doi.org/10.1007/s13202-021-01298-9>
- [9] Elmaadawy KG, El Hassan MM, Sallam AM. Rock Typing and Reservoir Quality Analysis of the Abu Madi Reservoir: Distribution Prediction Using Artificial Neural Networks in the West El Manzala Area, Onshore Nile Delta, Egypt. *Arabian Journal for Science and Engineering*, 2024; 49(1): 913-44. <https://doi.org/10.1007/s13369-023-08403-6>
- [10] Al-Dujaili AN, Shabani M, AL-Jawad MS. Lithofacies and electrofacies models for Mishrif Formation in West Qurna oilfield, Southern Iraq by deterministic and stochastic methods (comparison and analyzing). *Petroleum Science and Technology*, 2024; 42(13):1656-84. <https://doi.org/10.1080/10916466.2023.2168282>
- [11] Osung WE, Onyekuru SO, Ikoru DO, Akaolisa CC, Agbasi OE, Opara KD. Sequence stratigraphy of the foraminiferal zones F9700 and F9800 in the Niger Delta: A comprehensive litho-sequence approach. *Journal of African Earth Sciences*, 2024; 211: 105181. <https://doi.org/10.1016/j.jafrearsci.2024.105181>
- [12] Newsham KE, Rushing JA. An integrated work-flow model to characterize unconventional gas resources: part I—geological assessment and petrophysical evaluation. In *SPE Annual Technical Conference and Exhibition*, 2001 (pp. SPE-71351). SPE. <https://doi.org/10.2118/71351-MS>
- [13] Chandra V, Barnett A, Corbett P, Geiger S, Wright P, Steele R, Milroy P. Effective integration of reservoir rock-typing and simulation using near-wellbore upscaling. *Marine and Petroleum Geology*, 2015; 67: 307-26. <https://doi.org/10.1016/j.marpetgeo.2015.05.005>
- [14] Gunter GW, Viro EJ, Wolgemuth K. Identifying value added opportunities by integrating well log interpretation, petrophysical rock types and flow units; introducing a new multi-component stratigraphic modified lorenz method. In *SPWLA Annual Logging Symposium 2012 Jun 16* (pp. SPWLA-2012). SPWLA.
- [15] FANG X, ZHU G, YANG Y, LI F, FENG H. Quantitative Method of Classification and Discrimination of a Porous Carbonate Reservoir Integrating K-means Clustering and Bayesian Theory. *Acta Geologica Sinica-English Edition*, 2023; 97(1): 176-89. <https://doi.org/10.1111/1755-6724.14941>
- [16] Pittman ED. Relationship of porosity and permeability to various parameters derived from mercury injection-capillary pressure curves for sandstone (1). *AAPG bulletin*. 1992; 76(2): 191-8. <https://doi.org/10.1306/BDF87A4-1718-11D7-8645000102C1865D>
- [17] Eftekhari SH, Memariani M, Maleki Z, Aleali M, Kianoush P. Hydraulic flow unit and rock types of the Asmari Formation, an application of flow zone index and fuzzy C-means clustering methods. *Scientific Reports*, 2024; 14(1): 5003. <https://doi.org/10.1038/s41598-024-55741-y>
- [18] Mirzaei-Paiaman A, Ostadhassan M, Rezaee R, Saboorian-Jooybari H, Chen Z. A new approach in petrophysical rock typing. *Journal of Petroleum Science and Engineering*, 2018; 166: 445-64. <https://doi.org/10.1016/j.petrol.2018.03.075>
- [19] Gunter GW, Finneran JM, Hartmann DJ, Miller JD. Early determination of reservoir flow units using an integrated petrophysical method. In *SPE Annual Technical Conference and Exhibition*, 1997 Oct 5 (pp. SPE-38679). SPE. <https://doi.org/10.2118/38679-MS>
- [20] Amaefule JO, Altunbay M, Tiab D, Kersey DG, Keelan DK. Enhanced reservoir description: using core and log data to identify hydraulic (flow) units and predict permeability in uncored intervals/wells. In *SPE annual technical conference and exhibition*. OnePetro, 1993. <https://doi.org/10.2118/26436-MS>
- [21] Orodu OD, Tang Z, Fei Q. Hydraulic (flow) unit determination and permeability prediction: a case study of block Shen-95, Liaohe Oilfield, North-East China. *Journal of Applied Sciences*, 2009; 9(10): 1801-16. <https://doi.org/10.3923/jas.2009.1801.1816>
- [22] Zhang Y, Bao Z, Yang F, Mao S, Song J, Jiang L The controls of pore-throat structure on fluid performance in tight clastic rock reservoir: a case from the upper Triassic of Chang 7 Member, Ordos Basin, China. *Geofluids*, 2018; 1-17. <https://doi.org/10.1155/2018/3403026>
- [23] Paustian R, Andersson L, Helland JO, Wildenschild D. On the relationship between capillary pressure, saturation, and interfacial area for three-phase flow in water-wet porous media. *Advances in Water Resources*, 2021; 151: 103905. <https://doi.org/10.1016/j.advwatres.2021.103905>

- [24] Al-Dujaili AN, Shabani M, AL-Jawad MS. Effect of heterogeneity on capillary pressure and relative permeability curves in carbonate reservoirs. A case study for Mishrif formation in West Qurna/1 Oilfield, Iraq. *Iraqi Journal of Chemical and Petroleum Engineering*, 2023; 24(1): 13-26. <https://doi.org/10.31699/IJCPE.2023.1.3>
- [25] Schön J. *Physical properties of rocks: A workbook* (Vol. 8). Elsevier, 2011.
- [26] Al-Jinaay HM, Jaber MF. Applied NMR Log Technology to Determine Reservoir Characterization and Flow Units for the Mishrif Formation in Buzurgan Field Southeast Iraq. *Journal of Physics: Conference Series*, 2019; 1294(8): 082003). <https://doi.org/10.1088/1742-6596/1294/8/082003>
- [27] Alhusseini AK, Hamd-Allah S. Estimation of initial oil in place for Buzurgan Oil Field by using volumetric method and reservoir simulation method. *The Iraqi Geological Journal*, 2022: 108-22. <https://doi.org/10.46717/igj.55.2C.9ms-2022-08-22>
- [28] AlHusseini AK, Hamd-Allah S. Rock facies classification and its effect on the estimation of original oil in place based on petrophysical properties data. *International Journal of Nonlinear Analysis and Applications*, 2023; 14(1): 527-40. <https://doi.org/10.22075/ijnaa.2022.6855>
- [29] Abdulkareem AN, Mashloosh MJ, Hussein RA, Mohammed MI. Reservoir simulation of Mishrif formation in Buzurgan oil field. *AIP Conference Proceedings*, 2023; 2809(1). <https://doi.org/10.1063/5.0143478>
- [30] Al-Baldawi BA. Integrated Core and Log Data to Determine the Reservoir Flow Unit and Rock Facies for Mishrif Formation in South Eastern Iraq. *The Iraqi Geological Journal*, 2023: 118-34. <https://doi.org/10.46717/igj.56.1F.9ms-2023-6-17>
- [31] Sun X, Qiao Z, Guo R, Zhu G, Zhang J, Shao G, & Xu Z. Lithofacies, architecture and evolution of carbonate tidal delta system: implications for reservoir heterogeneity (Mid-Cretaceous Mishrif Formation, Southeast Iraq). *Marine and Petroleum Geology*, 2024; 106912. <https://doi.org/10.1016/j.marpetgeo.2024.106912>
- [32] Liu Y, Liu Y, Zhang Q, Li C, Feng Y, Wang Y, & Ma H. Petrophysical static rock typing for carbonate reservoirs based on mercury injection capillary pressure curves using principal component analysis. *Journal of Petroleum Science and Engineering*. 2019; 181, 106175. <https://doi.org/10.1016/j.petrol.2019.06.039>
- [33] Al-Dujaili AN. Reservoir rock typing and storage capacity of Mishrif Carbonate Formation in West Qurna/1 Oil Field, Iraq. *Carbonates and Evaporites*. 2023;38(4):83. <https://doi.org/10.1007/s13146-023-00908-3>
- [34] Mohsin M, Tavakoli V, Jamalain A. The effects of heterogeneity on pressure derived porosity changes in carbonate reservoirs, Mishrif formation in SE Iraq. *Petroleum Science and Technology*, 2023; 41(8), 898-915. <https://doi.org/10.1080/10916466.2022.2070210>
- [35] Mahdi TA, Aqrawi AA. Sequence stratigraphic analysis of the mid-cretaceous Mishrif Formation, southern Mesopotamian basin, Iraq. *Journal of petroleum geology*, 2014; 37(3): 287-312. <https://doi.org/10.1111/jpg.12584>
- [36] Idan RM, Salih AL Reservoir Quality Related to Diagenetic Development in the Carbonate Mishrif Formation: A Case Study from the X Oilfield, Southern Iraq. *The Iraqi Geological Journal* 2023; 100-114. <https://doi.org/10.46717/igj.56.2C.8ms-2023-9-14>
- [37] Kashnikov Y, & Ashikhmin S. Rock mechanics in the development of hydrocarbon fields. *Monograph.-Moscow, Mining Book PH*. 2019; 496.
- [38] Tobia FH, Aswad KJ. Petrography and geochemistry of Jurassic sandstones, Western Desert, Iraq: implications on provenance and tectonic setting. *Arabian Journal of Geosciences*, 2015; 8: 2771-2784. <https://doi.org/10.1007/s12517-014-1392-0>
- [39] Shyaa YF, Al-Rahim AM. Updating subsurface image of Khashim Al-Ahmer Gas Field using the interpretation for anisotropic velocity model North-Eastern Iraq. *The Iraqi Geological Journal*, 2021; 110-9. <https://doi.org/10.46717/igj.54.2F.10ms-2021-12-27>
- [40] Abdullah FH, El Gezeery T. Organic geochemical evaluation of hydrocarbons in Lower Cretaceous Middle Minagish reservoir, Kuwait. *Marine and Petroleum Geology*, 2016; 71: 41-54. <https://doi.org/10.1016/j.marpetgeo.2015.12.005>
- [41] Wohlwend S, Hart M, Weissert H. Chemostratigraphy of the Upper Albian to mid-Turonian Natih Formation (Oman)-how authigenic carbonate changes a global pattern. *The Depositional Record*, 2016; 2(1): 97-117. <https://doi.org/10.1002/dep2.15>
- [42] Tsusaka K, Fuji T, Shaver MA, Yudhia DP, Toma M, Al Ali SA, Toki T, Couzigou E, Matsubuchi H. Geomechanical Modeling Based on the First Success of Micro-Frac Tests in the Nahr Umr Formation in Offshore Abu Dhabi. In *Abu Dhabi International Petroleum Exhibition and Conference 2021 Dec 9* (p. D041S120R002). SPE. <https://doi.org/10.2118/207653-MS>

- [43] Khalil R. Grain-size analysis of middle cretaceous sandstone reservoirs, the Wasia formation, Riyadh province, Saudi Arabia. *Sustainability*, 2023; 15(10): 7983. <https://doi.org/10.3390/su15107983>
- [44] James GA, Wynd JG. Stratigraphic nomenclature of Iranian oil consortium agreement area. *AAPG bulletin*, 1965; 49(12): 2182-245. <https://doi.org/10.1306/A663388A-16C0-11D7-8645000102C1865D>
- [45] Alsharhan AS, Kendall CG. Precambrian to Jurassic rocks of Arabian Gulf and adjacent areas: their facies, depositional setting, and hydrocarbon habitat. *AAPG bulletin*, 1986; 70(8): 977-1002. <https://doi.org/10.1306/94886650-1704-11d7-8645000102c1865d>
- [46] Mohammed MM, Salih HM, Mnaty KH. 3D reservoir modeling of Buzurgan oil field, southern Iraq. *Iraqi Journal of Science*, 2022; 596-607. <https://doi.org/10.24996/ijs.2022.63.2.16>
- [47] Archie GE. Introduction to petrophysics of reservoir rocks. *AAPG bulletin*, 1950; 34(5): 943-61. <https://doi.org/10.1306/3D933F62-16B1-11D7-8645000102C1865D>
- [48] Al Kattan W, Jawad SN, Jomaah HA. Cluster analysis approach to identify rock type in Tertiary Reservoir of Khabaz oil field case study. *Iraqi Journal of Chemical and Petroleum Engineering*, 2018; 19(2):9-13. <https://doi.org/10.31699/IJCPE.2018.2.2>
- [49] Al-Jawad SN, Saleh AH, Al-Dabaj AA, Al-Rawi YT. Reservoir flow unit identification of the Mishrif formation in North Rumaila Field. *Arabian Journal of Geosciences*, 2014; 7: 2711-28. <https://doi.org/10.1007/s12517-013-0960-z>
- [50] Gomes JS, Ribeiro MT, Strohmenger CJ, Naghban S, Kalam MZ. Carbonate reservoir rock typing-the link between geology and SCAL. In Abu Dhabi international petroleum exhibition and conference 2008 Jan 1. Society of Petroleum Engineers. <https://doi.org/10.2118/118284-MS>
- [51] Ramadhan AA, Jaber AA, Zughar SS. Capillary pressure determination an Iraqi carbonate reservoir-Shuaiba reservoir/Khabaz field/North of Iraq. *AIP Conference Proceedings*, 2022; . 2443(1). <https://doi.org/10.1063/5.0092015>
- [52] Al-Jawad SN, Saleh AH. Flow units and rock type for reservoir characterization in carbonate reservoir: case study, south of Iraq. *Journal of Petroleum Exploration and Production Technology*, 2020; 10(1): 1-20. <https://doi.org/10.1007/s13202-019-0736-4>

To whom correspondence should be addressed: Dr. Ahmed N. AL-Dujaili, Amirkabir University of Technology/ Petroleum Engineering Department, No. 350, Hafez Ave, Valiasr Square, Tehran, Postal code: 1591634311, I.R. Iran, E-mail: ahmed.noori203@aut.ac.ir